

Proximity Effects in Monolayer Films: Kinetic Analysis of Amide Bond Formation at the Air–Water Interface Using ^1H NMR Spectroscopy

Jaya K. Kumar[†] and John S. Oliver*

Contribution from the Department of Chemistry, Box H, Brown University,
Providence, Rhode Island 02912

Received November 12, 2001

Abstract: The kinetics of amide bond formation in a monolayer film has been studied by proton NMR spectroscopy. Compression of a hexadecyl thioester of *N*-acetyl glycine (**1**) and a hexadecyl amide of glycine (**2**) at the air–water interface produces a single dipeptide product (**4**) that remains at the surface once formed. Extraction of the reaction mixture from the interface, followed by ^1H NMR spectroscopy, provides quantitative data on the rate of product formation. The kinetics of this reaction was examined as a function of surface pressure, subphase pH, and temperature. The monolayer provides an effective molarity for the reaction of ~ 500 M as compared to the bimolecular reaction of **1** and **4** in chloroform solution. The first-order rate constant for the reaction of **1** and **2** in the monolayer is less than 70-fold slower than k_{cat} for condensation of the first amide bond in the enzymatic synthesis of the cyclic antibiotic gramicidin S by gramicidin S synthetase. Activation energies of the reaction were extracted from the temperature dependence of the rate constants of the reaction and are 9.9 ± 1.0 and 2.1 ± 0.2 kcal/mol for the chloroform solution and monolayer reactions, respectively. The $\text{p}K_{\text{a}}$ of **2** in the monolayer was estimated to be ~ 0.5 $\text{p}K_{\text{a}}$ units lower than that of related amines in solution. The lower $\text{p}K_{\text{a}}$ at the interface as compared to that in solution may be ascribed to increased electrostatic repulsion at the interface relative to solution. The rate of reaction in the monolayer was also followed by monitoring changes in surface area as a function of time. The rate constant for the reaction of **1** and **4** as determined by changes in surface area differs significantly from the rate determined by NMR. The results indicate that measurements of surface area versus time may yield erroneous rate constants for reactions in monolayers.

Introduction

A high-resolution crystal structure of the 50S ribosome subunit was recently solved.¹ The structure reveals that the ribosome peptidyl transferase center is composed entirely of RNA, thus providing conclusive evidence that peptidyl transferase is a ribozyme. The crystal structure reveals details of the organization of the catalytic site. However, the mechanism employed by the ribosome to catalyze peptide bond formation remains unclear.²

The amino acid substrates used in ribosome-catalyzed peptide biosynthesis are activated species. The aminoacyl linkage of a typical acyl-tRNA is susceptible to nucleophilic attack, having a free energy of hydrolysis comparable to that of ATP.³ At the same time, the α -amino group of the attached amino acid is a good nucleophile. It is therefore conceivable that accurate

proximal alignment of the peptidyl-tRNA and an acyl-tRNA by the ribosome contributes significantly to the rate of peptide bond formation.⁴

Our interest in the design of nonenzymatic models of ribosomal and nonribosomal⁵ peptide synthesis led us to investigate the possible contribution of substrate proximity effects in the spontaneous catalysis of peptide bond formation. Amphiphilic molecules suspended at the air–water interface will form films of unimolecular thickness. The surface density and packing of these monolayer films can be controlled by varying the surface area available to the film. We reasoned that a monolayer surface would be an ideal model system to investigate amino acid condensation given the ease with which molecular orientation, surface pressure, and intermolecular distance can be controlled.

Langmuir–Blodgett films and monolayers increasingly are being used in the development of surfaces with novel properties.⁶ Materials for Langmuir–Blodgett films can be tailor-made via the design of both the head and the tail groups.⁷ Langmuir–Blodgett films allow unique opportunities for controlling molecular architecture as well as for providing high effective

* To whom correspondence should be addressed. Telephone: 401-863-2844. Fax: 401-863-2594. E-mail: John_Oliver@brown.edu.

[†] Present address: Department of Biological Chemistry and Molecular Pharmacology, Harvard Medical School, Boston, MA 02115.

- (1) Ban, N.; Nissen, P.; Hansen, J.; Moore, P. B.; Steitz, T. A. *Science* **2000**, *289*, 905.
- (2) (a) Nissen, P.; Hansen, J.; Ban, N.; Moore, P. B.; Steitz, T. A. *Science* **2000**, *289*, 920. (b) Muth, G. W.; Ortoleva-Donnelly, L.; Strobel, S. A. *Science* **2000**, *289*, 947. (c) Polacek, N.; Gaynor, M.; Yassin, A.; Mankin, A. S. *Nature* **2001**, *411*, 498.
- (3) Loftfield, R. B. *Prog. Nucleic Acid Res. Mol. Biol.* **1972**, *21*, 64.

- (4) (a) Krayevsky, A. A.; Kuhkhanova, M. K. *Prog. Nucleic Acid Res. Mol. Biol.* **1979**, *23*, 1. (b) Nierhaus, K. H.; Schulze, H.; Cooperman, B. S. *Biochem. Int.* **1980**, *1*, 185.
- (5) Doekel, S.; Marahiel, M. A. *Metab. Eng.* **2001**, *3*, 64.

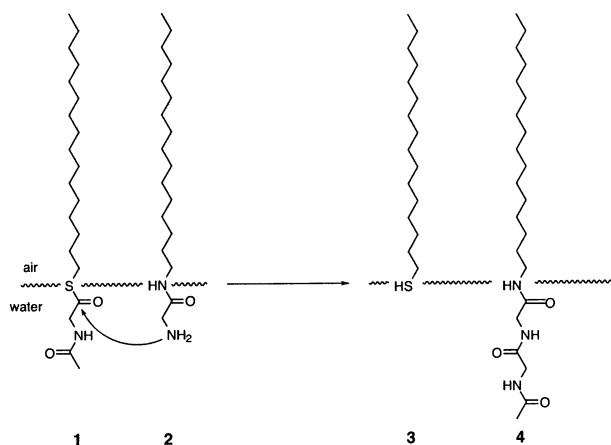


Figure 1. Reaction scheme of derivatized amino acids designed to give a discrete product at the air–water interface.

molarities of reactive groups.⁸ Proximity effects from concentrating reactive functionalities in a two-dimensional plane can result in rate accelerations of reactions over similar conditions in homogeneous solution.⁹ In addition, imposing structural order over the monolayer film reduces the rotational and translational entropies of the surface molecules, giving rise to reaction pathways that can be different from pathways in solution.¹⁰ However, the mechanisms that underlie reactivity in monolayers are not well understood.

As a model for the amide bond-forming reaction catalyzed by the ribosome, we investigated the behavior of a related system in a monolayer film. We have previously shown that a long chain thioester of an amino acid spontaneously undergoes an acyl transfer reaction with an amphiphilic nucleophile when the two reactants are held in proximity in a monolayer (see Figure 1).¹¹ To quantify the rate acceleration provided by proximity effects within the monolayer film, we now report the kinetics of this amide bond-forming reaction at the air–water interface.

The kinetics of reaction of several surface bound amphiphiles has been investigated. However, the majority of published studies monitor reactions at the air–water interface using surface techniques such as changes in surface area, surface pressure, surface potential, viscosity, or surface spectroscopy.¹² These methods are inadequate for structural characterization of reaction products, and the product/reactant ratios can only be obtained indirectly. Only a small number of investigations have employed

solution techniques such as chromatography for product characterization and kinetic analysis of reactions in monolayer films.¹³ To our knowledge, there is no report where a technique capable of structure determination has been utilized to unambiguously identify reaction products and provide quantitative measurements of reaction yield and kinetics at the air–water interface.

The components of a reaction designed to form a discrete product at the air–water interface are shown in Figure 1. A monolayer composed of **1** and **2** is formed on an aqueous subphase. The thioester **1** is the single reactive electrophile, and the amino group of **2** is the only nucleophile present in the monolayer. The condensation products of this reaction, dipeptide **4** and thiol **3**, remain at the interface after the reaction. The N-terminus of **1** is derivatized, precluding further reaction.

In our initial report on this reaction, the monolayer film was isolated from the air–water interface, and the reaction products, including dipeptide **4**, were characterized by thin-layer chromatography, mass spectrometry, FT-IR, and ¹H NMR spectroscopy.¹¹

We have developed protocols that allow us to use ¹H NMR spectroscopy to evaluate product formation of single compression experiments on a Langmuir–Blodgett film trough. This allows accurate measurement of reaction progress at each time point analyzed. Herein, we describe the effect of pH, surface pressure, and temperature on the kinetics of an amide bond-forming reaction at the air–water interface.

Experimental Section

General. The synthesis and characterization of **1**, **2**, and **4** have been described earlier.¹¹ CDCl₃ used to collect surface products was filtered through NaHCO₃ and Na₂SO₄ immediately prior to use. All chemicals used in buffering the subphase were molecular biology grade obtained from Sigma. Water was purified with a Millipore Nanopure system to a resistivity of at least 18 MΩ cm.

Hydrophobic Derivatization of Glass Slides. Clean microscope slides were subjected to the RCA cleaning method.¹⁴ The slides were first immersed in a boiling solution of H₂O/H₂O₂/NH₄OH (5:1:1) for 10 min and then in a boiling solution of H₂O/H₂O₂/HCl (6:1:1) for 10 min. The slides were rinsed with water and then dried overnight in an oven at 180 °C. The clean slides were derivatized by immersion in a solution of octadecyltrichlorosilane in hexadecane (2%) for 2 h.¹⁵ The slides were rinsed with CHCl₃ and dried under a stream of N₂. The derivatized slides were stored in a dark desiccator prior to use.

Pressure–Area Isotherms. Pressure–area isotherms were obtained with a film balance equipped with a Wilhelmy platinum plate connected to a microelectronic feedback system for surface pressure control. The film trough was placed in a specially constructed polycarbonate cabinet to minimize dust exposure and to control the humidity. The temperature of the subphase was maintained by circulating water through the walls of the trough. The subphase pH was maintained by a buffered solution (10 mM NaOAc, 1 mM EDTA, 0.5 M NaCl). Amphiphiles were spread with a 50 μL syringe from ~1 mg/mL solutions in CHCl₃ by applying the solution to at least 10 different places on the water surface. For mixed monolayers, a chloroform solution containing the two amphiphiles was spread. Solvent was allowed to evaporate for 30 min. The monolayer was compressed at a speed of 3 × 10¹⁷ Å²/min.

Equilibrium Spreading Pressures. Equilibrium spreading pressures were measured by depositing 300 μL of ~1 mg/mL solutions of the

- (6) (a) Ostuni, E.; Chen, C. S.; Ingber, D. E.; Whitesides, G. M. *Langmuir* **2001**, *17*, 2828. (b) Xu, G. F.; Wang, W. X.; Groves, J. T.; Hecht, M. H. *Proc. Natl. Acad. Sci. U.S.A.* **2001**, *98*, 3652. (c) Mrksich, M. *Chem. Soc. Rev.* **2000**, *29*, 267. (d) Taton, T. A.; Mirkin, C. A.; Letsinger, R. L. *Science* **2000**, *289*, 1757. (e) Ricco, A. J.; Crooks, R. M. *Acc. Chem. Res.* **1998**, *31*, 200. (f) Mirkin, C. A.; Ratner, M. A. *Annu. Rev. Phys. Chem.* **1992**, *43*, 719.
- (7) Ulman, A. *An Introduction to Ultrathin Organic Films: From Langmuir–Blodgett to Self-Assembly*; Academic: New York, 1991.
- (8) Ahmad, J. *Langmuir* **1996**, *12*, 963.
- (9) (a) Bartz, M.; Kuther, J.; Seshadri, R.; Tremel, W. *Angew. Chem., Int. Ed.* **1998**, *37*, 2466. (b) Otto, S.; Engberts, J.; Kwak, J. C. T. *J. Am. Chem. Soc.* **1998**, *120*, 9517. (c) Tollner, K.; PopovitzBiro, R.; Lahav, M.; Milstein, D. *Science* **1997**, *278*, 2100.
- (10) (a) Yousaf, M. N.; Chan, E. W. L.; Mrksich, M. *Angew. Chem., Intl. Ed.* **2000**, *39*, 1943. (b) Jaeger, D. A.; Su, D.; Zafar, A.; Piknova, B.; Hall, S. B. *J. Am. Chem. Soc.* **2000**, *122*, 2749. (c) Ahmad, J.; Astin, K. B. *J. Am. Chem. Soc.* **1986**, *108*, 7434.
- (11) Oliver, J. S.; Singh, J. *J. Org. Chem.* **1997**, *62*, 6436.
- (12) (a) Peltonen, J. P. K.; Pingsheng, H.; Linden, M.; Rosenholm, J. B. *J. Phys. Chem.* **1994**, *98*, 12403. (b) Bodalia, R.; Manzanares, J.; Reiss, H.; Duran, R. *Macromolecules* **1994**, *27*, 2002. (c) Paddeu, S.; Erokhin, V.; Nicolini, C. *Thin Solid Films* **1996**, *285*, 854.

- (13) (a) Ahmad, J. *Langmuir* **1996**, *12*, 963. (b) Valenty, S. J. *J. Am. Chem. Soc.* **1979**, *101*, 1.
- (14) Kern, W. *J. Electrochem. Soc.* **1990**, *137*, 1887.
- (15) Byrd, H.; Whipps, S.; Pike, J. K.; Ma, J.; Nagler, S. E.; Talham, D. R. *J. Am. Chem. Soc.* **1994**, *116*, 295.

amphiphiles on the subphase. The constant value of pressure attained over 3–12 h was recorded as the equilibrium spreading pressure.

Surface Reactions. Working solutions of equimolar **1** and **2** in CDCl_3 were prepared fresh each week. Working solutions were stored at -20°C between experiments. The concentration of the working solutions was 0.5–1.0 mg/mL. For kinetic runs, an aliquot of the working solution (20–40 μL , 30–50 nmol) was deposited on a buffered aqueous subphase in a Langmuir–Blodgett trough as described for obtaining isotherms. After evaporation of the solvent, the monolayer was compressed to the experimental surface pressure by movement of Teflon barriers at the aqueous surface at a speed of $3 \times 10^{17} \text{ \AA}^2/\text{min}$. Once the desired pressure was attained, it was held constant during the reaction by computer-controlled movement of the barriers. Reaction times varied from 5 min to 10 h, after which the monolayer was compressed rapidly to a minimum surface area allowed by the film trough barriers. The reaction mixture was lifted from the subphase with a hydrophobically coated glass slide. The material was recovered by washing the slide surface with CDCl_3 (500 μL) into an NMR tube. To complete recovery of material from the slide, the bottom 3 mm of the slide was broken off and immersed in the NMR tube for 3 h. The glass was removed, and the sample was analyzed by NMR. NMR acquisition times were from 12 to 23 h. The concentration of **1** and **2** during NMR data collection is 3–5 μM . The half-life of the second-order solution reaction at these concentrations is on the order of $5 \times 10^6 \text{ h}$ and thus does not interfere with the NMR analysis.

The subphase was maintained at a constant pH during the experiment with a sodium acetate buffer (10 mM NaOAc, 1 mM EDTA, 0.5 M NaCl). The potential involvement of the buffer as a general acid–base catalyst was checked by varying the concentration of sodium acetate over a range of 10–100 mM. No change of the reaction rate was observed at increased acetate concentration.

For variable temperature experiments, the film trough, filled with buffered subphase, was equilibrated for a minimum of 1 h prior to running reactions. The temperature of the subphase was checked immediately before compressing the surface active molecules.

Control experiments were performed to assess recoveries of reactants and products. Deposition of known amounts of dipeptide **4** followed by isolation from the monolayer showed that typical recoveries from the air–water interface were in excess of 90%. Separate control experiments, in which mixtures of known composition of starting material **2** and dipeptide **4** were deposited on and then recovered from an aqueous subphase, showed that there was no selective loss of one component of the reaction. Background hydrolysis of **1** in monolayers did not occur in the time frame of the experiments conducted in this study.

Solution Reactions. Stock solutions of **1** and **2** ($\sim 1 \text{ mg/mL}$) were prepared in CDCl_3 . A 1:1 molar mixture of the two reactants was transferred by syringe into NMR tubes fitted with screw caps and Teflon seals. The reaction was monitored by ^1H NMR spectroscopy.

NMR Analysis. ^1H NMR spectra were recorded using a 400 MHz spectrometer. The width of a $\pi/2$ pulse was determined by obtaining ^1H NMR spectra of a mixture of known composition of **1** and **2** in CDCl_3 and varying the pulse time to maximize the signal intensity. Delay times of sufficient length were included in all NMR experiments so that magnetization recovered completely to equilibrium between the pulses as judged from the integration of several different resonances in the spectra. The acquisition time was minimized by reducing the number of data points stored in the time domain (SI) from 64 to 32 K. The digital resolution of the spectrum (0.4 Hz/point) was sufficient for accurate integration of the signal intensities.

Results

Miscibility and Stability of the Reaction Components in the Monolayer. For the reaction shown in Figure 1 to proceed to any significant extent within the monolayer, the two reactants, **1** and **2**, must be miscible. Figure 2 shows pressure versus area

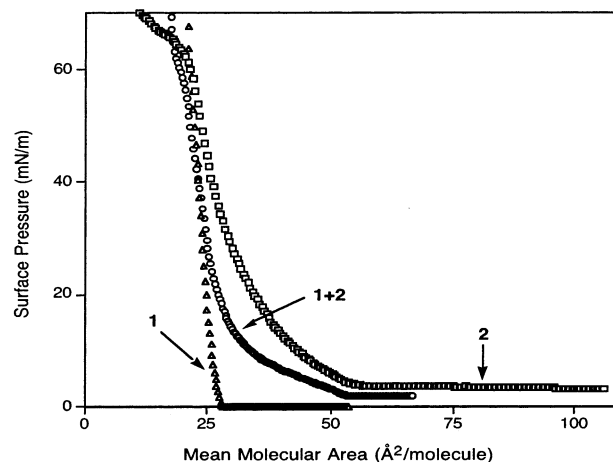


Figure 2. Pressure–area isotherms of **1**, **2**, and an equimolar mixture of **1** and **2** measured on an aqueous subphase at pH 7.8 and 22°C .

(π/A) isotherms of **1**, **2**, and an equimolar mixture of **1** and **2** measured on an aqueous subphase.

Each of the pure components has a high collapse pressure with departure from the maximum slope at surface pressures of 60–70 mN/m. Mean molecular areas of 23–25 \AA^2 at the collapse pressure are in agreement with literature values for amphiphiles with single hydrocarbon chains.¹⁶ The isotherm for the two component system indicates that the monolayer is a homogeneous mixture.¹⁷ The absence of a decrease from maximum slope at 65 mN/m for the mixture indicates that neither component is selectively extruded from the surface. A single collapse pressure as seen in the isotherm of the 1:1 mixture of **1** and **2** is also suggestive of a homogeneous mixed monolayer. The extent of reaction observed when the reaction is run to completion provides additional evidence that the monolayer is a single phase (see below).

Isotherms of mixtures of **1** and **2** were measured at each value of subphase pH used in kinetic runs. These isotherms establish that the monolayer is stable over this pH range. Figure 3 shows π/A isotherms of equimolar mixtures of **1** and **2** measured on buffered, aqueous subphases. The isotherms are similar in that they show almost identical phase changes with decreasing mean molecular area.

Equilibrium Spreading Pressures of Reaction Components. Equilibrium spreading pressures were measured for the individual starting materials **1** and **2**, products **3** and **4**, and a 1:1 mixture of **1** and **2**. The equilibrium surface pressures span the range of 19–36 mN/m (Table 1). Surface pressures higher than the equilibrium spreading pressure result in extrusion of surface material into the subphase or crystallization at the surface of one or more components from the surface over long periods of time. All reactions at the air–water interface were carried out at a surface pressure lower than the equilibrium spreading pressure of each of the components of the reaction so that the reactants and the products form stable films and are not extruded from the monolayer.

Kinetic Analysis and Rate Expression. During the reaction, the effective densities of materials at the air–water interface are high and essentially constant at the maximum extent of

(16) Mingotaud, A.-F.; Mingotaud, C.; Patterson, L. K. *Handbook of Monolayers*; Academic Press: San Diego, 1993.

(17) Gaines, G. L. *Insoluble Monolayers at Liquid–Gas Interfaces*; Interscience: New York, 1966.

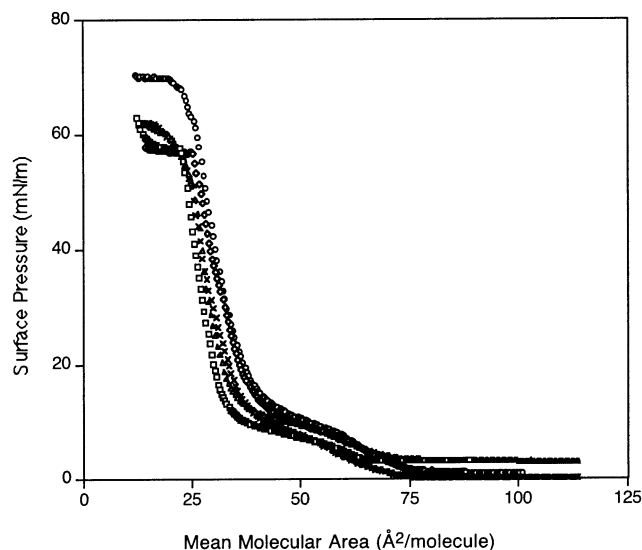


Figure 3. Pressure–area isotherms for 1:1 mixtures of **1** and **2** measured on an aqueous subphase (10 mM NaOAc, 1 mM EDTA, 0.5 M NaCl) at subphase pH 5.2 (×), pH 5.7 (O), pH 6.2 (Δ), pH 7.0 (◇), and pH 7.5 (□) at 22 °C.

Table 1. Equilibrium Spreading Pressures of Reaction Components at Room Temperature on a Subphase Maintained at pH 7.8

compound	equilibrium spreading pressure (mN/m)
nucleophile 2	36
electrophile 1	33
dipeptide 4	19
hexadecyl thiol 3	20
1:1 mixture of 1 and 2	22

reaction used in the experiments described here. Thus, the reaction is pseudo first order and the kinetic expression is



where A_T is the total amine (**2**) concentration, and k_{obs} is the observed rate constant. The reaction is pseudo first order with respect to $[A_T]$, so the rate law is

$$\ln([A_T]_0/[A_T]_t) = k_{\text{obs}}t \quad (2)$$

where $[A_T]_0$ is the initial amine concentration, and $[A_T]_t$ is the amine concentration at time t .

Because $[A_T]_0 \propto [1]_t + [4]_t$ and $[A_T]_t \propto [1]_t$, then the observed rate constant for the reaction can be determined without direct knowledge of the absolute concentration of components in the monolayer. The material isolated from the surface was analyzed by ^1H NMR. Integration of resolved resonances for **1** and **4** was used to calculate the ratio of $[A_T]_0/[A_T]_t$ at each time point.

The rate law for the true rate of the reaction can be written as

$$v = k_1[A_F] \quad (3)$$

where $[A_F]$ is the concentration of free amine **2**. The nucleophile **2** is in equilibrium with its protonated form which has a dissociation constant K_a .

$$v = k_1[A_T]K_a/(K_a + [\text{H}^+]) \quad (4)$$

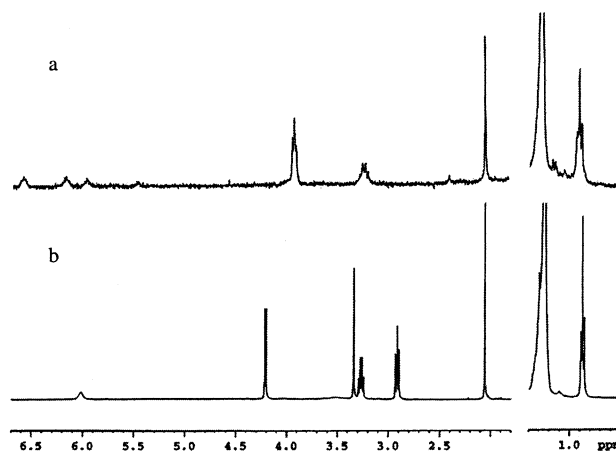


Figure 4. (a) ^1H NMR spectrum of compound **4** synthesized in solution. (b) ^1H NMR spectrum of an equimolar mixture of reactants **1** and **2**. Intensities of the resonances from the two $\alpha\text{-H}$'s in **1** (doublet at 4.21 ppm) and the four $\alpha\text{-H}$'s in the dipeptide product **4** (dd at 3.92 ppm) were integrated for analysis of reactions.

Thus, the observed rate constant (k_{obs}) is related to the true first-order rate constant (k_1) of the reaction by expression 5.

$$k_{\text{obs}} = k_1K_a/(K_a + [\text{H}^+]) \quad (5)$$

The K_a of **2** and k_1 for the reaction can be determined by measuring k_{obs} at multiple values of subphase pH and fitting the data to eq 5.

Reaction Kinetics. The kinetics of the reaction between **1** and **2** at the air–water interface was investigated at several values of subphase pH (5.2, 5.7, 6.2, 7.0, 7.5) at 22 °C. For each subphase pH, an equimolar mixture of **1** and **2** in CDCl_3 was deposited on a buffered aqueous subphase. After evaporation of the solvent, the monolayer was compressed to a surface pressure of 12 mN/m, and the surface pressure was maintained at this value during the reaction. After varying periods of reaction time, the monolayer was compressed rapidly to a minimum surface area, and the reaction mixture was lifted from the subphase by sweeping the surface with a hydrophobically coated glass slide. The material was recovered from the slide by washing with CDCl_3 .

NMR spectra for the starting materials **1** and **2** and for the dipeptide reaction product **4** are shown in Figure 4. The crude reaction mixtures isolated from the aqueous surface were analyzed for relative yields of **1** and **4** by ^1H NMR spectroscopy. Each reaction contained approximately 40 nmol of material. The intensities of the ^1H NMR resonances from the two $\alpha\text{-H}$'s in residual **1** (doublet at 4.21 ppm) and the four $\alpha\text{-H}$'s in the dipeptide product **4** (dd at 3.92 ppm) were separately integrated to afford product/reactant ratios. A typical set of experiments is shown in Figure 5. Each spectrum in the stack plot in Figure 5 was obtained from a surface reaction that had been allowed to react for the indicated time, after which the crude reaction mixture was isolated and subjected to NMR analysis as described in the Experimental Section.

Values of $\ln([A_T]_0/[A_T]_t)$, where $[A_T]_0$ is the initial concentration of **1**, and $[A_T]_t$ is the concentration at time t , were calculated from the integrated signal intensities of each ^1H NMR spectrum. The rate data at five different values of pH are plotted as $\ln([A_T]_0/[A_T]_t)$ versus time in Figure 6. The different values of $\ln([A_T]_0/[A_T]_t)$ observed at time zero at each pH are likely due

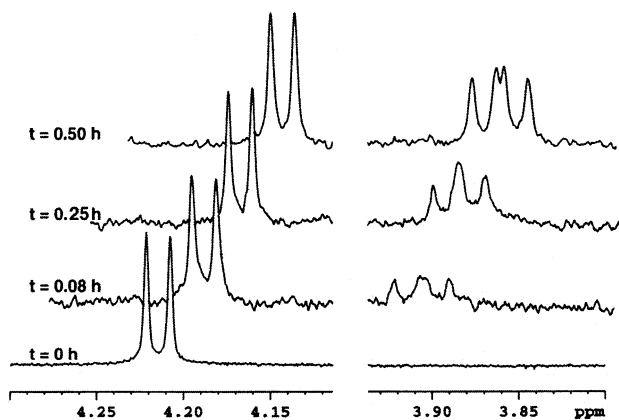


Figure 5. ^1H NMR spectra of reaction mixture extracted after reaction for different periods of time at the air–water interface on a subphase maintained at pH 7.0 and 22 °C. Intensities of the ^1H NMR resonances from the two $\alpha\text{-H}$'s in residual **1** (doublet at 4.21 ppm) and the four $\alpha\text{-H}$'s in the dipeptide product **4** (dd at 3.92 ppm) were integrated to afford product/reactant ratios.

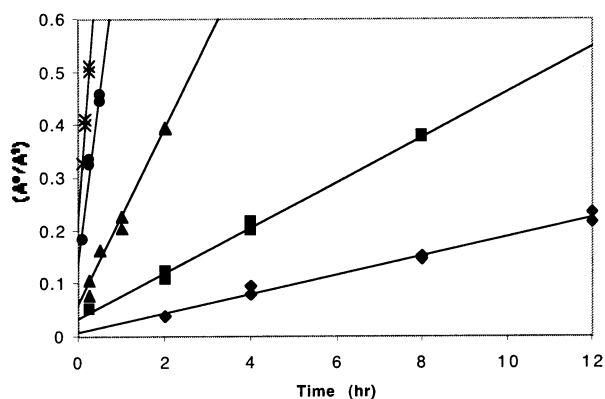


Figure 6. First-order plots for reactions at a constant surface pressure of 12 mN/m at 22 °C at subphase pH 5.2 (◆), pH 5.7 (■), pH 6.2 (▲), pH 7.0 (●), and pH 7.5 (*).

Table 2. Observed Rate Constants (k_{obs}) Obtained at Five Values of Subphase pH and at a Constant Surface Pressure of 12 mN/m ($T = 22$ °C, $\mu = 0.5$ M NaCl)

pH	k_{obs} (h^{-1})
5.2	0.018 ± 0.001
5.7	0.043 ± 0.001
6.2	0.166 ± 0.009
7.0	0.628 ± 0.055
7.5	1.076 ± 0.052

to background reaction that occurs as the monolayer is initially compressed to the reaction surface pressure of 12 mN/m. Pseudo first-order rate constants (k_{obs}) for the reaction were obtained from the slope of linear fits to the data in Figure 6 (Table 2).

As expected, the rate of reaction increased with increasing pH. The reaction was found to obey first-order kinetics up to at least 40% reaction as judged from the good fit of the data to a single exponential.¹⁸

Determination of the First-Order Rate Constant k_1 . To determine the first-order rate constant, k_1 , the values of k_{obs} and $[\text{H}^+]$ were used to fit eq 5 and solve for k_1 and K_a .¹⁹ Experimental data for k_{obs} and the calculated curve for the best fit to eq 5 are shown in Figure 7. The first-order rate constant

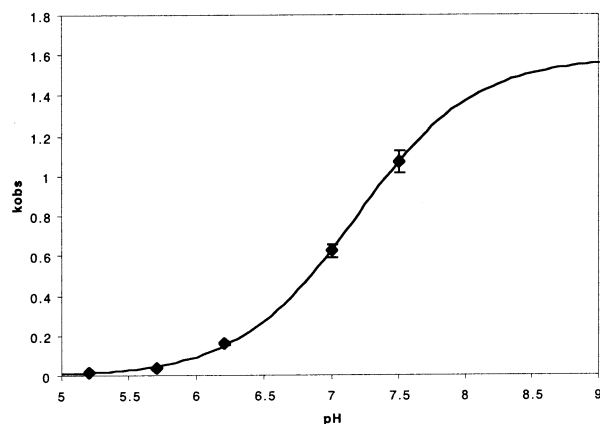


Figure 7. Plot of experimentally determined rate constants versus subphase pH. The data from Table 2 are plotted as filled diamonds (◆). The line is calculated from eq 5 using the experimentally determined values for k_1 and K_a .

was determined to be $1.58 \pm 0.07 \text{ h}^{-1}$. The solution reaction of **1** and **2** in CDCl_3 was followed by ^1H NMR spectroscopy. The second-order rate constant at 22 °C for the reaction in solution is $(3.0 \pm 0.3) \times 10^{-3} \text{ M}^{-1} \text{ h}^{-1}$.²⁰

The effective molarity of the reaction at the air–water interface, calculated as the ratio of the first-order rate constant of the reaction in the monolayer to the second-order bimolecular rate constant in solution, is ~ 500 M. The polarity at the interface is defined by the nature of the headgroup of the amphiphile. This redefines the microenvironment polarity, which may no longer be that of the bulk subphase.²¹ The choice of chloroform as the solvent for the solution reaction is based on the premise that the interface has an effective dielectric constant closer to an organic solvent than an aqueous solution. The effective molarities for similar reactions in solution, derived from ratios of inter- versus intramolecular reaction rate constants for aminolysis of thioesters, are on the order of ~ 22 M.²² Thus, the monolayer provides effective molarities greater than that obtained in related intramolecular reactions.

Determination of the $\text{p}K_a$ of **2 in Monolayers.** Titration curves of functional groups at interfaces are shifted relative to the titration curves in solution.²³ Alteration in $\text{p}K_a$'s provides additional opportunities for the design of reactions in monolayers. Thus, it is of interest to determine accurate values for the difference in functional group $\text{p}K_a$'s at an interface versus bulk solution. In general, it is more energetically disfavored to generate the ionized form of a functional group at the interface due to increased electrostatic repulsion and low effective dielectric constants.²⁴ Acid dissociation constants of amines have been reported to be between 0.5–5 $\text{p}K_a$ units lower at an interface as compared to solution. The wide variation in values for the $\text{p}K_a$ may result, in part, from the variety of experimental techniques such as contact angle measurements, surface titration, and the study of collapse pressure as a function of subphase pH that have been utilized to infer surface $\text{p}K_a$'s.²⁵

(18) At higher conversions, the resulting inhomogeneity in the composition of the monolayer does not permit analysis by first-order kinetics.

(19) Equation 5 can also be rearranged to a linear form to solve for k_1 and $\text{p}K_a$: $\log(A/(k_{\text{obs}} - 1)) = -\text{pH} + \text{p}K_a$.

(20) The bimolecular rate constant was determined at millimolar concentration of the two substrates, as this is the solubility limit of the two reactants and the product in chloroform-*d*.

(21) Mingotaud, C.; Chauvet, J. P.; Patterson, L. K. *Thin Solid Films* **1994**, *242*, 243.

(22) (a) Kirby, A. J. *Adv. Phys. Org. Chem.* **1980**, *17*, 183. (b) Searles, S.; Nukina, S. *J. Am. Chem. Soc.* **1965**, *87*, 5656.

(23) Bain, C. D.; Whitesides, G. M. *Langmuir* **1989**, *5*, 1370.

(24) (a) Holmes-Farley, S. R.; Bain, C. D.; Whitesides, G. M. *Langmuir* **1988**, *4*, 921. (b) Holmes-Farley, S. R.; Reamey, R. H.; McCarthy, T. J.; Deutch, J.; Whitesides, G. M. *Langmuir* **1985**, *1*, 725.

Table 3. Observed Rate Constants for Reactions at Different Surface Pressures on a Subphase Maintained at pH 5.7 and 22 °C

π (mN/m)	k_{obs} (s^{-1})
4	0.45×10^{-5}
12	1.19×10^{-5}
18	3.05×10^{-5}

The $\text{p}K_{\text{a}}$ of **2** was determined to be 7.18 ± 0.05 at 22 °C from the fit of the k_{obs} data to eq 5. The $\text{p}K_{\text{a}}$ of related amines in solution is between 7.6 and 8.0,²⁶ giving rise to a shift of 0.5–0.9 $\text{p}K_{\text{a}}$ units from the interface. The $\text{p}K_{\text{a}}$ of **2** determined in our experiments reflects the average $\text{p}K_{\text{a}}$ in the surface over the time course of the reaction. A monolayer composed of only **2** would likely result in a lower $\text{p}K_{\text{a}}$. The $\text{p}K_{\text{a}}$ would also be shifted to lower values as the surface pressure is increased into the condensed region at about 18 mN/m for the mixture of **1** and **2**.²⁷

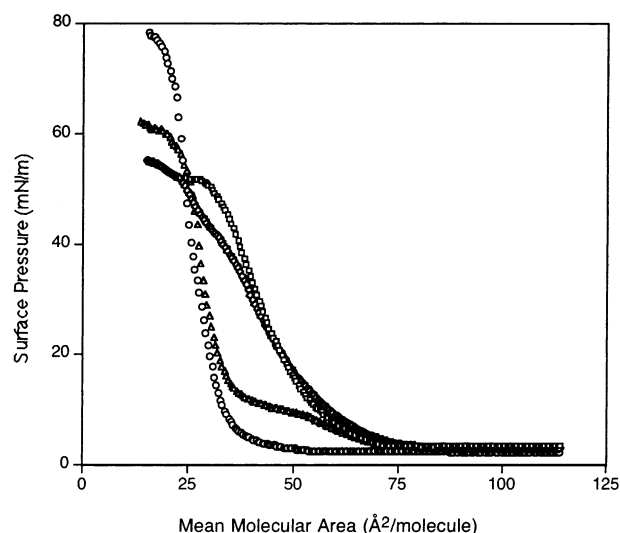
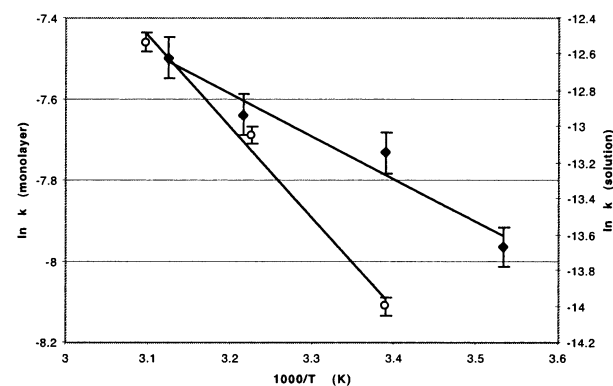
Effect of Surface Pressure on Reaction Rates. To ascertain the effect of surface pressure on the rate of reaction of **1** and **2** in the monolayer, rate constants were determined at several surface pressures at a subphase pH of 5.7. The observed rate constant increases with pressure in this range (Table 3).

The range of surface pressures of 4–18 mN/m represents a change in mean molecular area from 60 to 30 Å². The increased reaction rates observed upon reducing the mean molecular area by 50% are expected due to proximity effects and reduced translational and rotational entropies at the interface. The mole fraction of **2** present as the free amine at any subphase pH will also increase as the surface pressure increases, due to increasing electrostatic repulsion, resulting in an increased observed rate of reaction.

Temperature Dependence of Surface and Solution Reactions of **1 and **2**.** The temperature dependence of the rate constant for the reaction of **1** and **2** at the air–water interface was examined using NMR quantification of reaction progress to help clarify the basis of the rate acceleration observed for the monolayer reaction. Isotherms of the 1:1 mixture of **1** and **2** were measured over an aqueous, buffered subphase maintained at pH 6.2 over a temperature range of 10–47 °C (Figure 8). Increased thermal motion of the molecules leads to expansion of the monolayer film. This is manifested as an increase in surface pressure for phase transitions with an increase in temperature. At reduced temperatures, the monolayer is more condensed.

Rate constants (k_{obs}) for the reaction on a subphase of pH 6.2 at a constant surface pressure of 12 mN/m were determined at four different temperatures. The temperature dependence of the second-order rate constant k_2 for the corresponding bimolecular reaction of **1** and **2** in solution was also determined.

The rate constant k_1 for the monolayer reaction at the various temperatures can be estimated from k_{obs} . Assuming that the relative amount of ionized and neutral forms of amine **2** is independent of temperature, the ratio k_1/k_{obs} will be constant over the temperature range studied. In fact, the extent of ionization probably changes slightly as the temperature is varied.

**Figure 8.** Pressure–area isotherms for 1:1 mixtures of **1** and **2** measured on an aqueous subphase (10 mM NaO₂C₂H₃, 1 mM EDTA, 0.5 M NaCl) at 10 °C (○), 22 °C (△), 38 °C (◇), and 47 °C (□).**Figure 9.** Arrhenius plot for reaction at a constant surface pressure of 12 mN/m on a subphase maintained at pH 6.2 (◆). Arrhenius plot for reaction of **1** and **2** in CDCl₃ solution (○).**Table 4.** Activation Parameters Obtained from a Temperature Dependence Study of Rate Constants for the Reaction of **1** and **2** (a) on a Subphase Maintained at pH 6.2, (b) in CDCl₃ Solution

reaction	E_{a}^{a}	A^{b}	$\Delta H^{\ddagger \text{a}}$	$\Delta S^{\ddagger \text{c}}$
(a)	2.1 ± 0.2	$1.5 \pm 0.7 \times 10^{-2}$	1.5 ± 0.2	-69 ± 1
(b)	9.9 ± 1.0	22 ± 6	9.4 ± 1.0	-54 ± 3

^a In units of kcal/mol. ^b In units of s^{-1} for reaction in monolayer, and $\text{M}^{-1} \text{s}^{-1}$ for reaction in solution. ^c In units of $\text{cal K}^{-1} \text{mol}^{-1}$.

The $\text{p}K_{\text{a}}$ of glycylglycine falls 0.78 units as the temperature is changed from 10 to 40 °C.²⁸ However, at the pH of the experiment (6.2), the extent of ionization of **2**, with a $\text{p}K_{\text{a}}$ of 7.2, is high and will have a smaller variation as a function of temperature. At 22 °C and pH 6.2, the ratio of k_1/k_{obs} is 9.52.

The solution and surface reactions exhibit modest temperature dependence. Arrhenius plots for each reaction are shown in Figure 9. The activation parameters calculated from the rate versus temperature data for both reactions are shown in Table 4. The activation energies were calculated to be 9.9 and 2.1 kcal/mol for the chloroform solution and monolayer reactions, respectively. The difference in activation energies ($\Delta E_{\text{a}} = 7.8$

(25) (a) Vezenov, D. V.; Noy, A.; Rozsnyai, L. F.; Lieber, C. M. *J. Am. Chem. Soc.* **1997**, *119*, 2006. (b) An, S. W.; Thomas, R. K. *Langmuir* **1997**, *13*, 6881. (c) Wamser, C. C.; Gilbert, M. I. *Langmuir* **1992**, *8*, 1608.

(26) Perrin, D. D. *Dissociation Constants of Organic Bases in Aqueous Solution*; Butterworth: London, 1965.

(27) Wang, H.; Zhao, X.; Eisenthal, K. B. *J. Phys. Chem. B* **2000**, *104*, 8855.

(28) *Stability Constants of Metal-Ion Complexes, Supplement #1*; Sillen, L. G., Martell, A. E., Eds.; The Chemical Society: London, 1964.

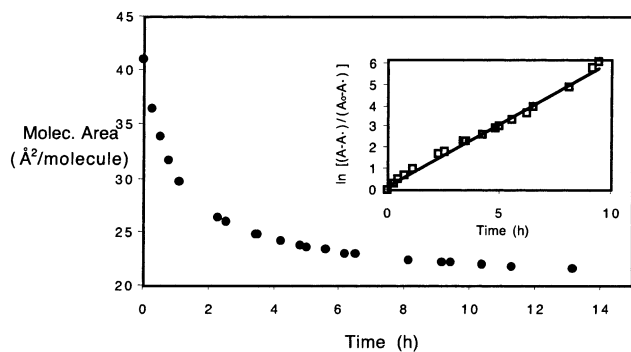


Figure 10. Change in mean molecular area as a function of time for the reaction of **1** and **2** at a constant surface pressure of 12 mN/m. The subphase was maintained at pH 6.2 and 22 °C. Inset: Plot of $\ln[(A - A_\infty)/(A_0 - A_\infty)]$ versus time for the reaction of **1** and **2**.

kcal/mol) for these two reactions reflects the higher rate of reaction in the monolayer (Table 4).

Reaction Rate Determined by the Change in Mean Molecular Area. The kinetics of reactions in monolayers is typically followed by measurement of a surface property such as the area of the film or the surface potential.¹² In particular, the variation of film area at constant surface pressure during a reaction is monitored as a function of time to infer kinetic parameters. The general expression for a reaction obeying first-order kinetics in solution has been modified for interfacial reactions as shown in eq 6.²⁹

$$(A - A_\infty)/(A_0 - A_\infty) = e^{-kt} \quad (6)$$

where A is the area of the film at any time t during the reaction, A_∞ is the area at $t = \infty$, and A_0 is the area at $t = 0$.

To determine the accuracy of rate constants obtained by surface measurements, we compared the rate of reaction of **1** and **2** in the monolayer as determined by NMR to the rate determined by following the change in surface area at a constant pressure. The reaction of **1** and **2** was carried out at subphase pH 6.2 and at a constant surface pressure of 12 mN/m (conditions identical to those for the original kinetic study at pH 6.2 by NMR). The mean molecular area (mma) was monitored as a function of time. A plot of mma versus time (Figure 10) shows an initial rapid decrease in mma that attains a near constant value in ~ 10 h. The value of the mma at that point is assumed to represent the end point of the reaction. There is a small but discernible slope for the plot at longer time, which represents changes in mma due to undetermined zero order effects. After correcting for this background rate, $\ln(A_0/A_t)$ versus time was plotted (Figure 10, inset). The slope of this plot afforded a pseudo first-order rate constant of $0.60 \pm 0.01 \text{ h}^{-1}$. The observed rate constant as determined from NMR measurements for the same reaction under identical conditions is $0.166 \pm 0.009 \text{ h}^{-1}$.

Discussion

It is well established that concentrating reactive functionalities in a two-dimensional plane results in rate accelerations over similar conditions in solution. However, the use of direct structural techniques to unambiguously identify reaction products and to accurately monitor the kinetics of reactions at

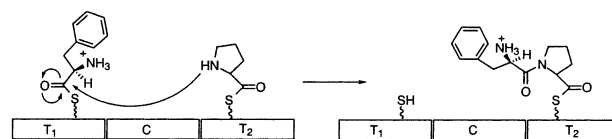


Figure 11. Cartoon of a condensation reaction to form an amide bond in gramicidin S synthetase. The C (condensation) domain mediates nucleophilic attack of proline, attached to the T₂ (thioester) domain, on D-phenylalanine, linked to the T₁ domain.

interfaces has been lacking. In this report, the kinetics of a reaction designed to yield a single dipeptide product upon compression of amino acid appended amphiphilic molecules at the air–water interface has been elucidated by the use of ¹H NMR spectroscopy. An equimolar mixture of a hexadecyl thioester of *N*-acetyl glycine and a hexadecyl amide of glycine forms a homogeneous self-assembled monolayer at the air–water interface. The ordered arrangement provides high effective molarities of reactive groups.

The kinetics of the reaction was monitored as a function of subphase pH. Comparison of the first-order rate constant for the reaction at 22 °C ($k_1 = 1.58 \text{ h}^{-1}$) in the monolayer to the second-order rate constant for the reaction in chloroform solution ($k_2 = 3 \times 10^{-3} \text{ M}^{-1} \text{ h}^{-1}$) affords an effective molarity of 500 M.

The rate acceleration of amide bond formation catalyzed by the monolayer results in a rate constant that is comparable to corresponding reactions in enzymes, this despite the fact that in the reaction described here, the reactants are not oriented by the surface to maximize reactivity.

Nonribosomal peptide synthetases catalyze the biosynthesis of a large number of small peptides. During loading of the peptide synthetases, amino acids are activated and linked to the protein as thioesters through enzyme bound 4'-phosphopantetheine (Ppant) on the T (thiolation) domain. Condensation of amino acids to form amide bonds occurs by nucleophilic attack of the amino group of one amino acid on the thioester of the aminoacyl-S-Ppant and is mediated by the C (condensation) domain.³⁰ One of the best characterized nonribosomal peptide synthetases is gramicidin S synthetase (Figure 11). The first translation/condensation step in gramicidin S synthetase generates D-Phe₁-L-Pro₂. The rate constant (k_{cat}) for this step is 1.8 min^{-1} (108 h^{-1}).³¹ This is a factor of less than 70-fold faster than the rate constant for condensation in the monolayer. The rate of the condensation reaction in the monolayer is further accelerated over 2.5-fold at slightly higher pressures (see Table 3).

The rate of the monolayer dependent reaction demonstrates the important role proximity can play in the biosynthesis of peptides. Progenitors of modern peptide forming enzymes, ribosomal, nonribosomal, or prebiotic, may have used the proximity effect exclusively to condense activated amino acids.

As compared to the bimolecular reaction in chloroform, the reaction in the monolayer has a more negative entropy of activation. The larger negative entropy of activation in the monolayer reaction may be a result of the development of charge in the transition state of this reaction. The polar nature of the transition state would be expected to result in reorganization of

(30) Stachelaus, T.; Mootz, H. D.; Bergendahl, V.; Marahiel, M. A. *J. Biol. Chem.* **1998**, *273*, 22773. (b) Stachelaus, T.; Marahiel, M. A. *J. Biol. Chem.* **1995**, *270*, 6163.

(31) Belshaw, P. J.; Walsh, C. T.; Stachelaus, T. *Science* **1999**, *284*, 486.

(29) MacRitchie, F. *Chemistry at Interfaces*; Academic Press: San Diego, 1990.

solvent or monolayer molecules in the boundary layer resulting in constrained orientations of neighboring molecules.

The monolayer reaction exhibits a significantly lower enthalpy of activation as compared to the reaction in chloroform. The most significant role of the monolayer in accelerating this reaction may be to increase the mole fraction of reactants present in a near attack conformation (NAC).³² The more preorganization imposed by the monolayer along the reaction path, the larger the population of reactive NACs. It has been shown that the stability of NACs in solution, and thus the mole fraction of conformations present as NACs, is enthalpically controlled. Our results indicate that the monolayer has effectively stabilized the NAC for the amide bond-forming reaction, thus lowering the enthalpy required to bring the reacting atoms together.

The acid dissociation constant of amphiphile **2** was determined to be 7.18 p*K*_a units at the air–water interface. This increased acidity of **2** at the air–water interface as compared to the p*K*_a of related amines in solution is in accord with reported shifts in p*K*_a of amines determined by contact angle measurements as well as surface titrations.²⁴ The shift in p*K*_a may be attributed to increased electrostatic repulsions and low dielectric constants at interfaces versus solution.

The rate constant of the reaction as determined by changes in surface area over a 10 h period is $0.60 \pm 0.01 \text{ h}^{-1}$ when run on a subphase of pH 6.2. Under identical conditions, the NMR data gave an observed rate constant of $0.166 \pm 0.009 \text{ h}^{-1}$. The NMR data to determine *k*_{obs} were obtained at reaction times up

to 2 h. When the change in surface area as a function of time is analyzed over the same time period, the observed rate constant is $0.89 \pm 0.05 \text{ h}^{-1}$. Thus, early rates as determined by surface area measurements are in greater discrepancy with the NMR experiment. The data indicate that the rate of reaction is not accurately determined by observing changes in surface area or other gross surface properties. The reasons for the discrepancy between the rates as measured by these two techniques are not known. However, nonadditivity of molecular areas of products and reactants may not be a valid assumption for this reaction, thus precluding the use of surface area to infer reaction progress. The results suggest that caution must be used in determining the kinetic behavior of surface films by observing surface properties.

In summary, we have demonstrated the utility of characterizing products of reactions for elucidating the kinetic pathways of reactions in monolayer films. The time, pH, surface pressure, and temperature dependence of an amide bond-forming reaction have been systematically explored.

Acknowledgment. This research was supported in part by the National Science Foundation under grant No. MCB-9508066. We also thank Prof. R. G. Lawler and Dr. J. Epp for help with NMR spectroscopy.

Supporting Information Available: NMR spectra for calculation of reaction kinetics (PDF). This material is available free of charge via the Internet at <http://pubs.acs.org>.

(32) (a) Lightstone, F. C.; Bruce, T. C. *Acc. Chem. Res.* **1999**, *32*, 127. (b) Lightstone, F. C.; Bruce, T. C. *Bioorg. Chem.* **1998**, *26*, 193.

JA0175237